International Journal of Heat and Mass Transfer 52 (2009) 3645–3653

Contents lists available at ScienceDirect

International Journal of Heat and Mass Transfer

journal homepage: www.elsevier.com/locate/ijhmt

Flow boiling in horizontal flattened tubes: Part II – Flow boiling heat transfer results and model

Jesús Moreno Quibén [a,b], Lixin Cheng [a,c], Ricardo J. da Silva Lima [a], John R. Thome [a,*]

[a] Laboratory of Heat and Mass Transfer (LTCM), Faculty of Engineering (STI), École Polytechnique Fédérale de Lausanne (EPFL), Station 9, CH-1015 Lausanne, Switzerland
[b] Wolverine LDA, Apartado 21-4740 Esposende, Portugal
[c] School of Engineering, University of Aberdeen, King's College, Aberdeen, AB24 3UE Scotland, UK

ARTICLE INFO

Article history:
Received 26 November 2008
Accepted 17 December 2008

Keywords:
Flow boiling
Heat transfer
Flattened tube
Experiments
Flow patterns
Flow pattern map
Model
R22
R410A

ABSTRACT

Experiments of flow boiling heat transfer were conducted in four horizontal flattened smooth copper tubes of two different heights of 2 and 3 mm. The equivalent diameters of the flattened tubes are 8.6, 7.17, 6.25, and 5.3 mm. The working fluids were R22 and R410A. The test conditions were: mass velocities from 150 to 500 kg/m^2 s, heat fluxes from 6 to 40 kW/m^2 and saturation temperature of 5 °C. The experimental heat transfer results are presented and the effects of mass flux, heat flux, and tube diameter on heat transfer are analyzed. Furthermore, the flow pattern based flow boiling heat transfer model of Wojtan et al. [L. Wojtan, T. Ursenbacher, J.R. Thome, Investigation of flow boiling in horizontal tubes: Part I – A new diabatic two-phase flow pattern map, Int. J. Heat Mass Transfer 48 (2005) 2955–2969; L. Wojtan, T. Ursenbacker, J.R. Thome, Investigation of flow boiling in horizontal tubes: Part II – Development of a new heat transfer model for stratified-wavy, dryout and mist flow regimes, Int. J. Heat Mass Transfer 48 (2005) 2970–2985], using the equivalent diameters, were compared to the experimental data. The model predicts 71% of the entire database of R22 and R410A ±30% overall. The model predicts well the flattened tube heat transfer coefficients for R22 while it does not predicts well those for R410A. Based on several physical considerations, a modified flow boiling heat transfer model was proposed for the flattened tubes on the basis of the Wojtan et al. model and it predicts the flattened tube heat transfer database of R22 and R410A by 85.8% within ±30%. The modified model is applied to the reduced pressures up to 0.19.

1. Introduction

Compared to a circular tube, a flattened tube has a higher internal surface area-to-cross-sectional flow area ratio, which can potentially be used to enhance the heat transfer rate and increase the compactness of the heat exchanger. Furthermore, flattened heat transfer tubes can greatly reduce the refrigerant charge in direct-expansion evaporators and condensers. Additionally, external potential advantages of flattened tube profiles are reduced air-side pressure drop and increase air-side heat transfer. So far, there are very limited studies on two-phase flow and heat transfer in flattened tubes in the literature. Wilson et al. [1] investigated refrigerant charge, two-phase pressure drop and heat transfer during condensation of two refrigerants R134a and R410A in several flattened tubes. Their results show significant reduction in refrigerant mass as a tube is flattened. They also indicate enhancement of condensation heat transfer and increase of pressure drop in the flattened tubes. Krishnaswamy et al. [2] investigated condensation heat transfer of steam–air mixtures in a horizontal flattened tube. They also proposed a simple heat transfer model. Their model predicts their data satisfactorily. Koyama et al. [3] conducted experiments on two-phase pressure drop and heat transfer of condensation of refrigerant R134a in multi-port extruded flattened tubes with hydraulic diameters of 1.114 and 0.807 mm. They concluded that to establish a prediction method of the pressure drop and heat transfer characteristics of pure refrigerant condensing in a small diameter tube, more experimental data for small diameter tubes should be investigated by considering the following terms: (1) flow patterns, (2) the effect of tube diameter, and (3) the interaction effect among the vapor shear stress and the gravitational acceleration and the surface tension. As for flow boiling in flattened tubes, however, there is no study available in the literature. In order to design a flattened tube evaporator, it is important to understand and predict the two-phase flow and flow boiling heat transfer characteristics inside horizontal tubes. In particular, in the case of a flattened tube having a very small height, the confinement of such a tube greatly affects two-phase and flow boiling heat transfer characteristics [4–7]. In Part II, experimental results of flow boiling heat transfer are presented and analyzed.

* Corresponding author. Tel.: +41 21 693 5981; fax: +41 21 693 5960.
E-mail addresses: jmoreno@wolverine.com.pt (J.M. Quibén), lixincheng@hotmail.com (L. Cheng), ricardo.lima@epfl.ch (R.J. da Silva Lima), john.thome@epfl.ch (J.R. Thome).

0017-9310/$ - see front matter © 2009 Elsevier Ltd. All rights reserved.
doi:10.1016/j.ijheatmasstransfer.2008.12.033

Nomenclature

A_L	cross-sectional area occupied by liquid phase (m^2)
c_p	specific heat at constant pressure (J/kg K)
D	internal tube diameter (m)
F	nucleate boiling correction factor
G	total vapor and liquid two-phase mass flux (kg/m^2 s)
h	heat transfer coefficient (W/m^2 K)
k	thermal conductivity (W/m K)
M	molecular weight (kg/kmol)
Pr	Prandtl number (=$c_p\mu/k$)
p	pressure (Pa)
p_r	reduced pressure (=p/p_{crit})
q	heat flux (W/m^2)
Re_V	vapor phase Reynolds number (=$GxD_e/\mu_V\varepsilon$)
Re_δ	liquid film Reynolds number (=$4G(1-x)\delta/\mu_L(1-\varepsilon)$)
T	temperature (°C)
t	tube wall thickness (m)
x	vapor quality
Greeks	
δ	liquid film thickness (m)
ε	cross-sectional vapor void fraction
μ	dynamic viscosity (N s/m^2)
θ	angle of tube perimeter (rad)
ρ	density (kg/m^3)
σ	standard deviation (%)
ξ	relative error (%)
$\overline{\xi}$	average error (%)
$\lvert\overline{\xi}\rvert$	mean error (%)
Subscripts	
cb	convective boiling
crit	critical
dry	dry
e	equivalent
IA	intermittent to annular flow
L	liquid
nb	nucleate boiling
sat	saturation
tp	two-phase flow
V	vapor
w	wall
wet	wetted
wi	inside wall
wo	outside wall

Furthermore, a modified flow pattern based heat transfer model for these flattened tubes was proposed for R410A and R22 flow boiling in the flattened tubes.

Flow patterns are very important in understanding the very complex two-phase flow phenomena and heat transfer trends in flow boiling [8]. Flow patterns at diabatic conditions are intrinsically related to the corresponding flow boiling heat transfer characteristics. The flow patterns can be used to explain physically the heat transfer mechanisms and characteristics. Over the past years, a number of flow pattern based flow boiling heat transfer models for various fluids were developed in LTCM. One of the earliest such kind of models is the Kattan–Thome–Favrat flow boiling heat transfer model [9–11] which was developed based on experimental data of R134a, R123, R502, R402A, and R404A in horizontal smooth tubes. The model predicts local heat transfer coefficients based on the local flow patterns and has methods for predicting heat transfer coefficients in the annular, intermittent, stratified-wavy and stratified flow regimes. Later on, Wojtan et al. [12,13] extended the Kattan–Thome–Favrat [9–11] flow map to include a new dryout region, new mist flow regime transition and subdivided the stratified-wavy regime into three sub-regimes (slug, stratified-wavy and slug, and stratified-wavy flows) based on their observations and dynamic void fraction measurements for R22 and R410A. They also developed the corresponding heat transfer methods for these flow regimes. Cheng et al. [14,15] developed a new flow map and a new flow boiling heat transfer model for CO_2 evaporation using the model of Wojtan et al. [12,13] as their starting point. Furthermore, new data allowed an updated flow map and heat transfer model to be proposed for CO_2 [16,17]. These models generally predict their respective flow boiling heat transfer data well. Recently, da Silva Lima et al. [18] compared the model of Wojtan et al. to their new flow boiling heat transfer data for R134a at three saturation temperatures, mass fluxes and two heat fluxes and found the model predicted their new data well. Furthermore, da Silva Lima et al. [19] compared their flow pattern observation with ammonia for a wide range of conditions the flow pattern map of Wojtan et al. and found that the map worked well for ammonia. Therefore, in the present study, the flow map and heat transfer model of Wojtan et al. were used to identify the flow regimes and to compare to the experimental heat transfer data in the flattened tubes.

2. Test setup and conditions

The test facility, test tubes, test section, measurement system and uncertainties are described in Part I. Flow boiling heat transfer coefficients of R22 and R410A were measured in the flattened tubes for the range of mass velocities from 150 to 500 kg/m^2 s, heat fluxes from 6 to 40 kW/m^2 and saturation temperature of 5 °C. This corresponds to reduced pressures p_r of 0.12 for R22 and 0.19 for 410A, respectively. Table 1 shows the test flattened tube number and dimensions (refer to Fig. 3 in part I). For each test run, these parameters were manually controlled to achieve desired test conditions. The measurements obtained with a National Instruments data acquisition system were monitored through a Personal Computer. Each experimental point resulted from the average of 10 acquisition cycles. Each acquisition cycle corresponds to an average from 100 acquisitions made in approximately 0.02 s. All measurements were made at steady state conditions.

3. Data reduction and test procedures

In the present study, the physical properties were obtained from REFPROP of NIST Version 6.01 [20]. The measurement and calculation of the local values of outside wall temperature T_{wo}, refrigerant saturation temperature T_{sat}, the local heat flux at the local measurement position q and vapor quality x are given in Part I of this study. With these measured parameters, the local flow boiling heat transfer coefficient can now be determined as

$$h_{tp} = \frac{q}{\overline{T}_{wi} - T_{sat}}, \tag{1}$$

Table 1
Flattened tube dimensions (mm).

Tube	H	W	t	D_e	D_h
Flattened tube No. 1	2	18.6	1.02	7.17	3.71
Flattened tube No. 2	3	17	0.76	8.6	5.35
Flattened tube No. 3	2	9.44	1.02	5.3	3.5
Flattened tube No. 4	3	7.87	0.86	6.25	4.88

where $\overline{T}_{wi}$ is the average value of the inside wall temperature at the measured cross-section, which is calculated according to one-dimension heat conduction in a flat wall for the flattened tubes as

$$\overline{T}_{wi} = \overline{T}_{wo} - \frac{qt}{k_w}, \tag{2}$$

where k_w is the thermal conductivity of copper, q is the heat flux based on the inside area of the flattened tube and $\overline{T}_{wo}$ is the average temperature of the measured outside wall temperatures at the local measurement position.

Due to the very small wall thickness and radius of the circular part of the flattened tubes, the inside wall temperature is also calculated using Eq. (2). The uncertainty of the heat transfer coefficient is ±6%.

4. Experimental results and analysis

Before the flow boiling tests of the two refrigerants in the flattened tubes, single phase liquid energy balance and turbulent heat transfer tests in two circular tubes with internal diameters of 8 and 13.84 mm were performed to validate the measurement system in the present study. The validation results were presented in Part I.

4.1. Flow boiling heat transfer experimental results

The effects of various parameters such as mass flux, heat flux, and tube equivalent diameter on the flow boiling heat transfer coefficients are presented and analyzed here.

Figs. 1 and 2 show the effect of mass flux on the flow boiling heat transfer coefficients in the four flattened tubes for R22 and R410A, respectively. It can be seen that the heat transfer coefficient increases with increasing mass flux in the flattened tubes for both refrigerants at most vapor qualities while this effect is not significant at very low vapor qualities. With increasing mass flux, convective boiling dominates heat transfer at higher vapor qualities. At very low vapor qualities, nucleate boiling is the dominant heat transfer mechanism and thus the effect of mass flux becomes weak. Mass flux also has a significant effect on the onset of dryout indicated by the peak in the heat transfer coefficients. For the same conditions, onset of dryout occurs earlier at higher mass fluxes. Furthermore, it can be seen that R410A has higher flow boiling heat transfer coefficients than R22 in the same flattened tube at the same test conditions. This is because R410A has higher latent heat, liquid and vapor conductivities, liquid and vapor specific heats but a lower surface tension than R22. All these physical properties have significant effects on nucleate boiling and convective boiling heat transfer. Thus, R140A has higher nucleate boiling and convection heat transfer coefficients than R22, resulting in higher flow boiling heat transfer coefficients.

Figs. 3 and 4 shows the effect of heat flux on flow boiling heat transfer coefficients for R22 and R410A, respectively. It can be seen that heat flux has a significant effect for both refrigerants. This effect becomes stronger at lower vapor qualities because nucleate boiling is the dominant heat transfer mechanism at lower vapor qualities. Furthermore, heat flux has strong effect on the onset of

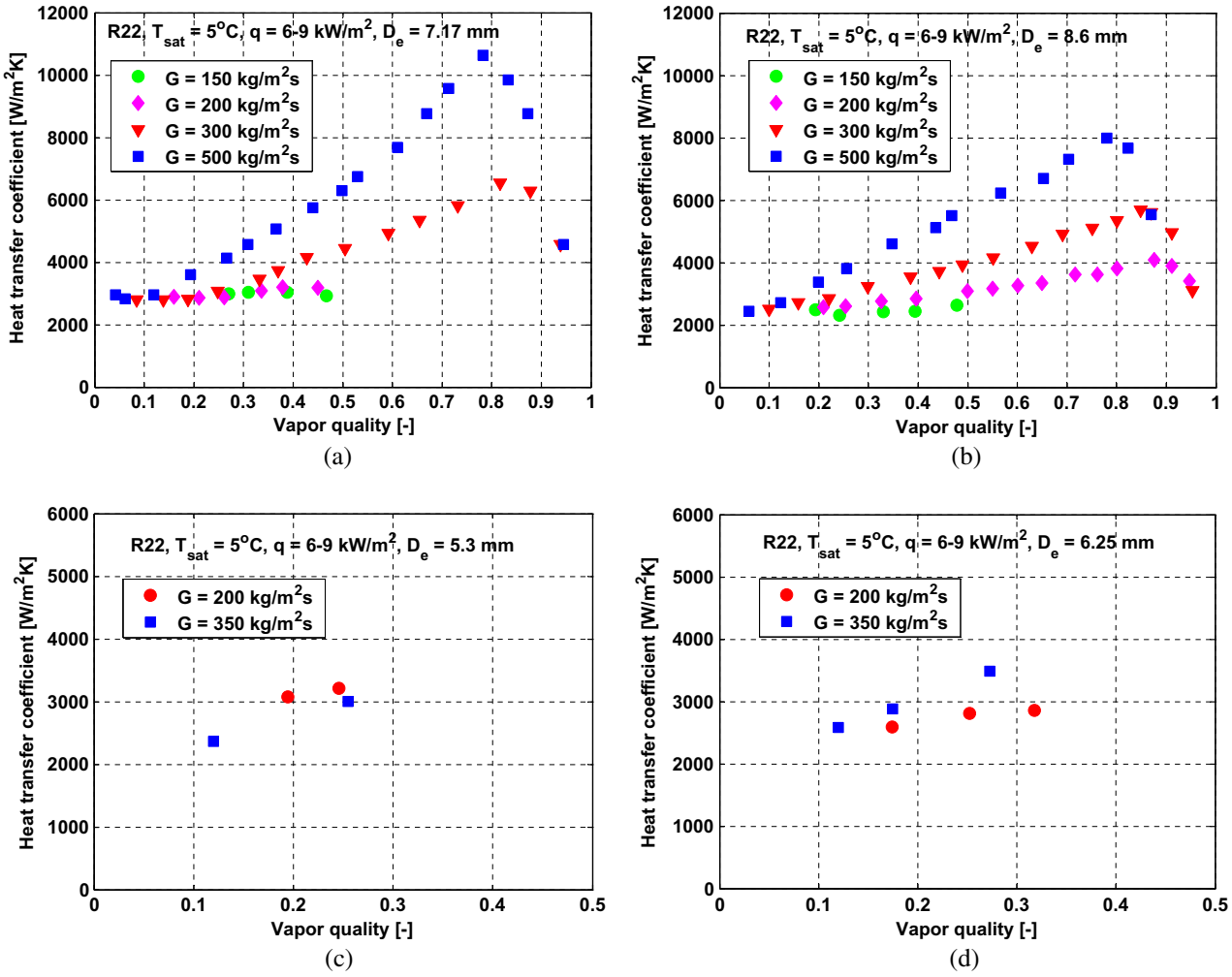

Fig. 1. The effect of mass flux on flow boiling heat transfer coefficient for R22: (a) Tube No. 1, (b) Tube No. 2, (c) Tube No. 3, and (d) Tube No. 4.

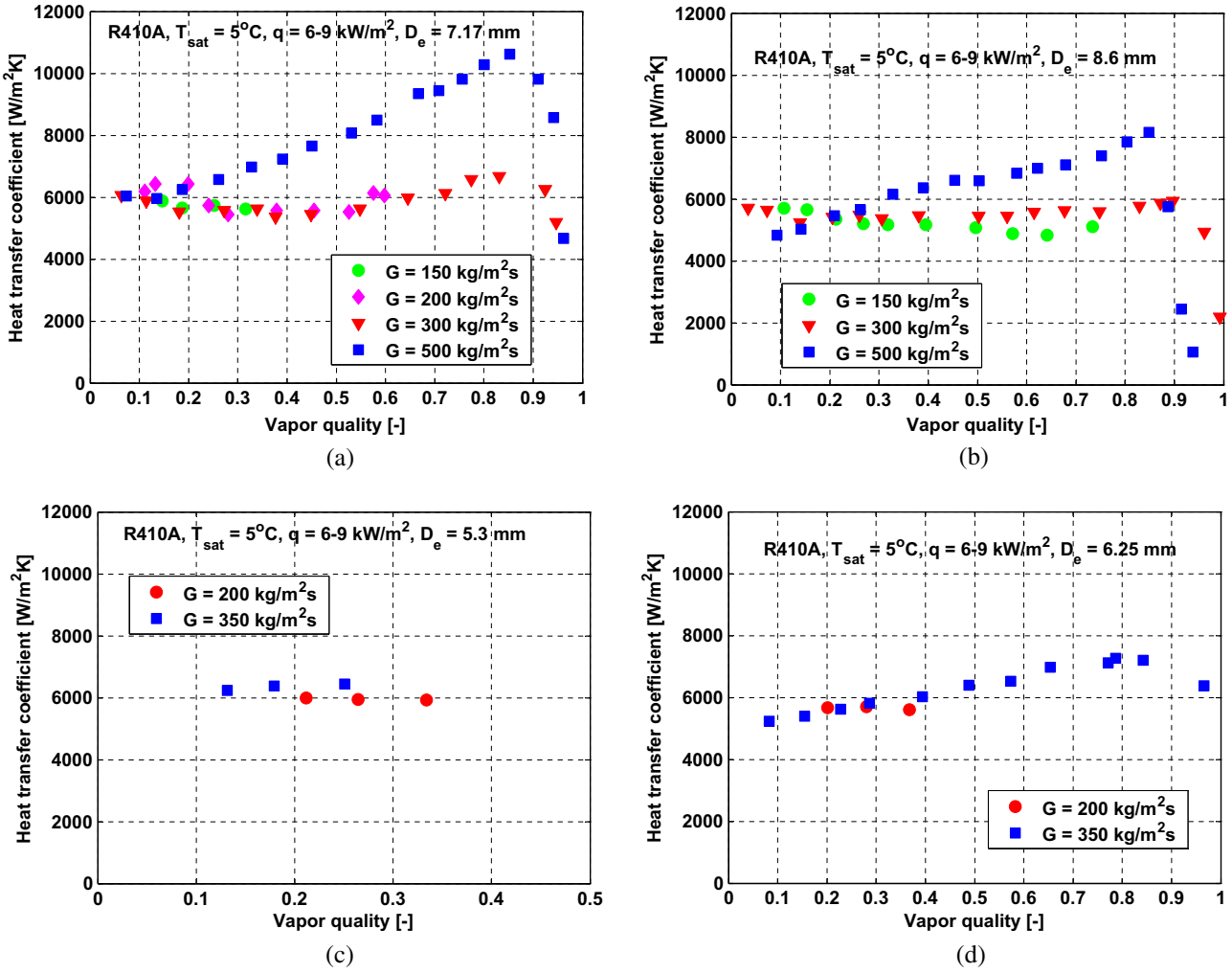

Fig. 2. The effect of mass flux on flow boiling heat transfer coefficient for R410A: (a) Tube No. 1, (b) Tube No. 2, (c) Tube No. 3, and (d) Tube No. 4.

dryout. With increasing heat flux, the onset of dryout occurs much earlier. This is consistent with the experimental results of several refrigerants in the circular tubes of Wojtan et al. [12,13].

Fig. 5(a) and (b) shows the effect of channel height on the heat transfer coefficients in the flattened tubes for the same test conditions. In general, heat transfer coefficient increases with decreasing tube equivalent diameter. However, it should be noted that the heat transfer coefficient differences for the similar tube equivalent diameters (e.g. D_e = 7.17 and 8.6 mm or D_e = 5.3 and 6.25 mm) are significant although the change in the equivalent diameter is small. The reason is possibly because of the effect of the channel heights of 2 and 3 mm. In general, confined channels (spaces) can increase nucleate boiling and convective heat transfer as has been shown by the studies of Bonjour and Lallemand [21,22]. Cheng et al. [4] also summarized the studies of the effect of confined channels on nucleate boiling heat transfer. Notably, both heights are within the microscale range according to the definition of Kandlikar [7]. The flattened channels should affect the two-phase flow regimes significantly; however the flow regime observations in sight-glasses were not possible for these confined channels due to the safety but should be investigated when a safe solution is found in the future.

4.2. Comparison of the experimental data to the flow pattern based heat transfer model of Wojtan et al.

Since the same working fluids as those used by Wojtan et al. [12,13] were tested for the flattened tubes in this study, the Wojtan et al. flow pattern based flow boiling heat transfer model is selected to compare to the flattened tube experimental heat transfer data here. The flow pattern map of Wojtan et al. [12,13] is used to identify the flow regimes in the flattened tubes. As mentioned by Cheng et al. [14–17], for non-circular channels, equivalent diameters rather than hydraulic diameters should be used in the flow pattern map. Using the equivalent diameter gives the same mass velocity as in the non-circular channel and thus correctly reflects the mean liquid and vapor velocities, something using a hydraulic diameter in a two-phase flow does not. The equivalent diameter is also used in the flow boiling heat transfer model. The details of the flow map and flow boiling heat transfer model can be found in Wojtan et al. [12,13]. No equations are given here for the sake of simplicity. It should be mentioned here that a number of flow boiling heat transfer correlations have been developed so far. For example, Yu et al. [23] investigated flow boiling heat transfer of R134a, R123, R22, R114, and R12 in two horizontal smooth copper tubes of 7.9 and 8.4 mm I.D., using water heated double-tube type test sections which are similar to these in the presented study. They proposed a new heat transfer correlation considering the surface effect for flow boiling in annular and semi-annular flow regimes and their correlation predicted well the experimental data. In the present study, all the flow regimes are considered. Therefore, only the flow patterned based heat transfer model by Wojtan et al. is used for the comparisons in the present study.

Fig. 6 shows the comparison of the entire flow boiling heat transfer database of R22 and R410A (Of the total 355 data points,

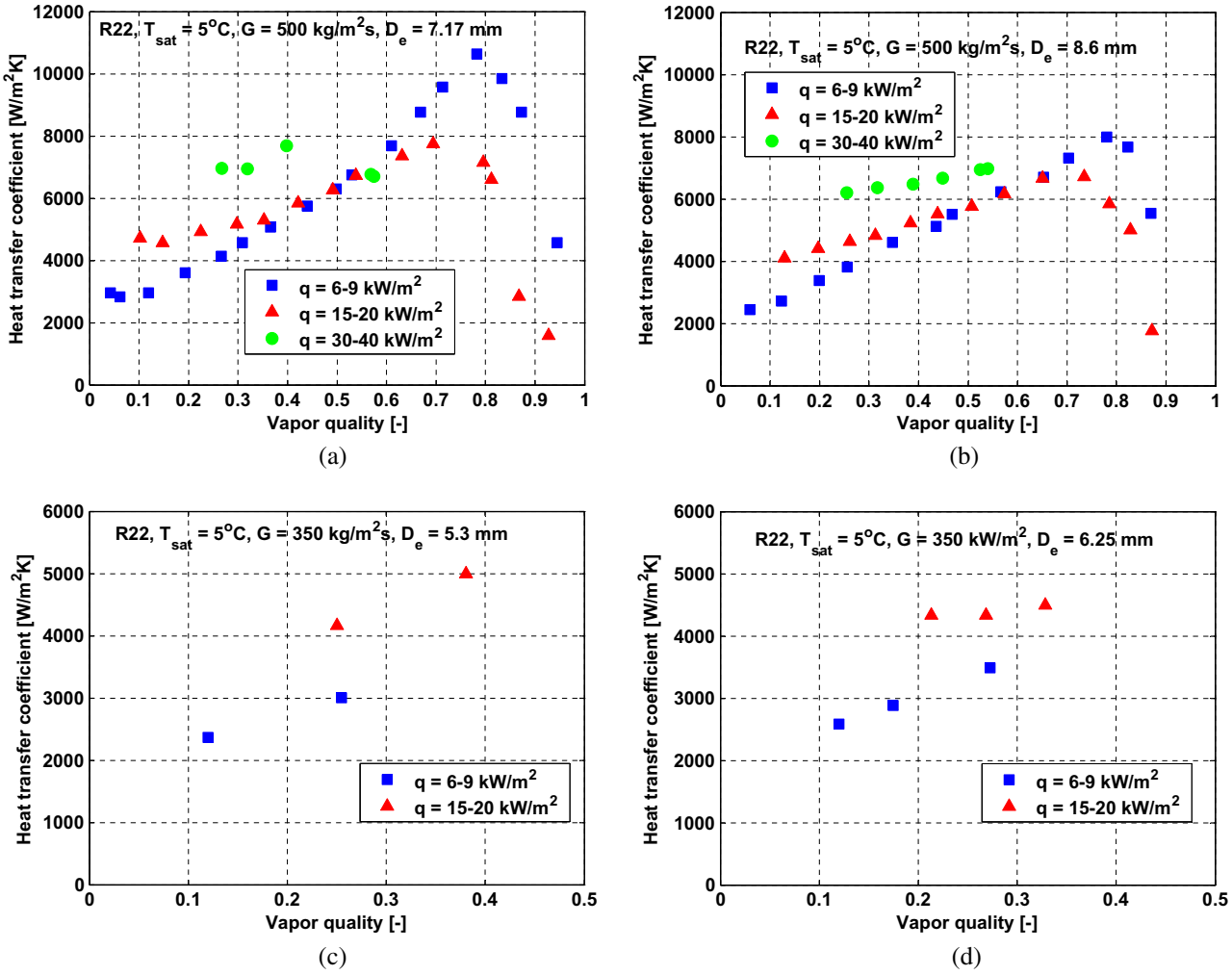

Fig. 3. The effect of heat flux on flow boiling heat transfer coefficient for R22: (a) Tube No. 1, (b) Tube No. 2, (c) Tube No. 3, and (d) Tube No. 4.

162 data points are for R22 and 193 data points are for R410A.) to the Wojtan et al. heat transfer model. The model predicts 71% of the entire database within ±30% overall as indicated in Table 2. It can be seen from Fig. 6 that the model predicts the flattened tube heat transfer data of R22 better than those of R410A. Statistically, the model predicts 87% of the R22 data within ±30% while it only predicts 57.5% of the R410A data within ±30%. Table 2 also summarizes the statistical analysis according to the flow patterns. The model works well in annular flow regime for the whole database of R22 and R410A except in other flow regimes. This is partly affected by the worse prediction for R410A. It should be noted that the heat transfer trend in the dryout region sharply changes and a small experimental error in the vapor quality due to the energy results in a very large error in heat transfer prediction in the dryout region. Thus, the predicted results for the dryout region are still reasonable. As for mist flow data, only five data points are available, so little can be concluded.

Fig. 7 shows the experimental and predicted flow boiling heat transfer coefficient ratios versus vapor qualities for the entire data base of R22 and R410A. The prediction for R22 is quite good in general and the prediction for annular flow regime data of R410A is good as well. However, the experimental data are much higher than the predicted values at lower vapor qualities $x \leqslant x_{IA}$ (in Slug-SW, SW, Slug and I flow regimes) for R410A, which apparently means that the nucleate boiling mechanism is enhanced applying the conventional theory. On the other hand, applying the micro-scale theory of Thome et al. [24] of the three zone model, this increase could also be explained by the promotion of thin film evaporation by the confinement of the bubbles. However, it is not clear why this only occurs for R410A. Therefore, a modified flow boiling heat transfer model is needed for the flattened tubes.

4.3. Modified flow boiling heat transfer model for the flattened tubes

The flow boiling heat transfer model of Wojtan et al. was modified for the flattened tubes according to the experimental data. The idea of the modification is based on the fact of the enhancement of nucleate boiling of R410A in the flattened tubes. This might be affected by combined function of the fluid physical properties and the channel confined heights. One, for instance, can imagine that the bubble frequency in nucleate boiling is increased by the higher crossflow shear in narrow channel. Therefore, a correction factor for the nucleate boiling heat transfer coefficients is proposed. Considering that most of the underpredicted data points are in the flow regimes at $x \leqslant x_{IA}$, this kind of modification seems reasonable and also simple to implement.

The Kattan–Thome–Favrat [9–11] general equation for the local flow boiling heat transfer coefficients h_{tp} in a horizontal tube is used as the basic flow boiling expression:

$$h_{tp} = \frac{\theta_{dry} h_V + (2\pi - \theta_{dry}) h_{wet}}{2\pi}, \tag{3}$$

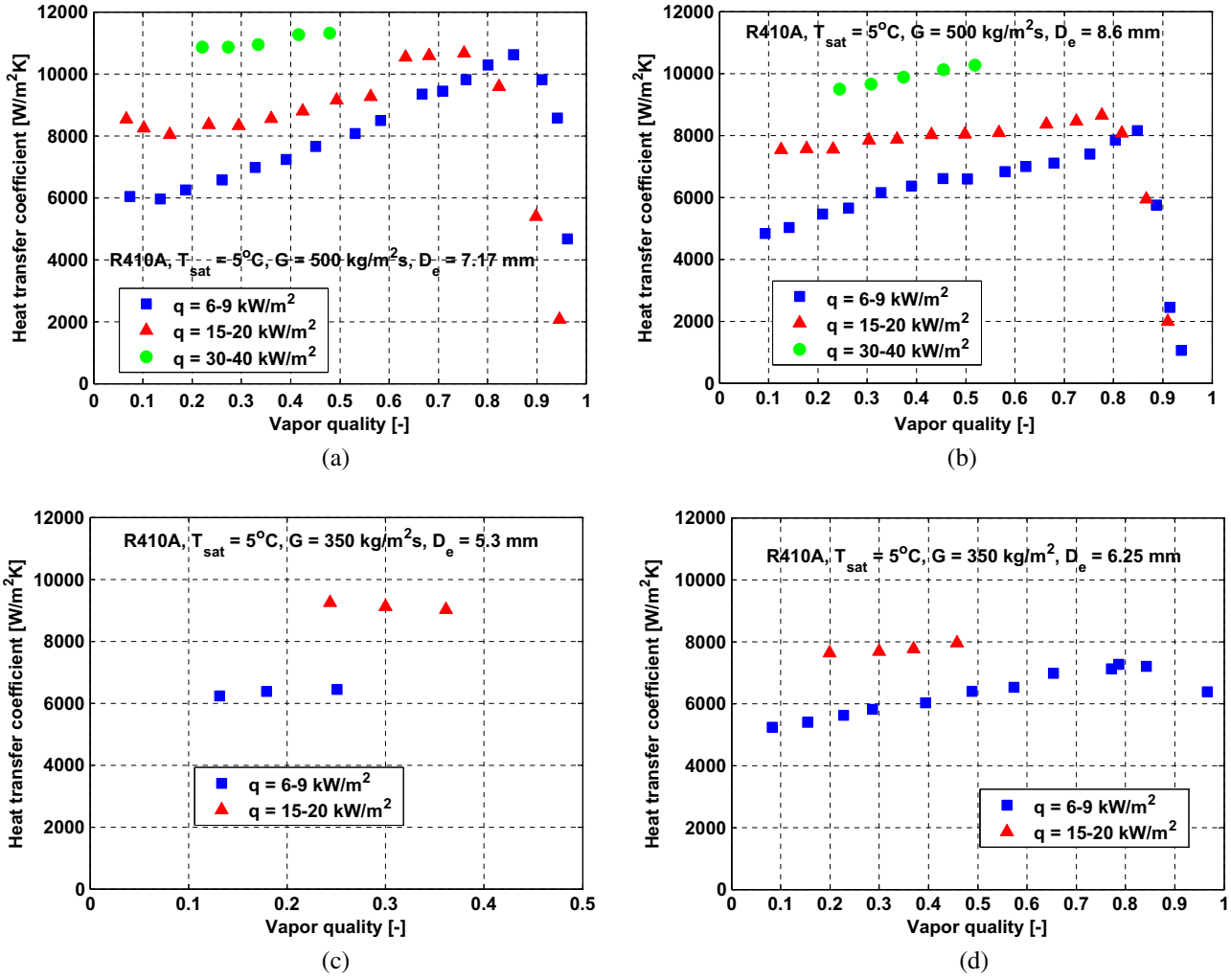

Fig. 4. The effect of heat flux on flow boiling heat transfer coefficient for R410A: (a) Tube No. 1, (b) Tube No. 2, (c) Tube No. 3, and (d) Tube No. 4.

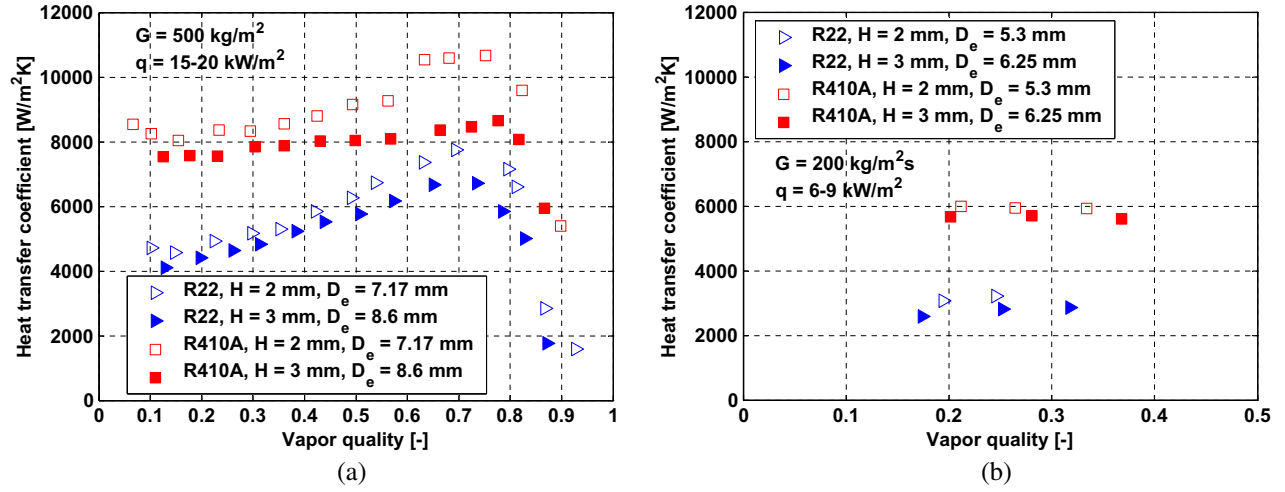

Fig. 5. The effect of channel height on flow boiling heat transfer coefficient for R22 and R410A: (a) $G = 500$ kg/m^2 s, $q = 15$–20 kW/m^2 and (b) $G = 200$ kg/m^2 s, $q = 6$–9 kW/m^2.

where θ_{dry} is the dry angle shown in Fig. 8. The dry angle θ_{dry} defines the flow structures and the ratio of the tube perimeter in contact with liquid and vapor. In stratified flow, θ_{dry} equals the stratified angle θ_{strat} [12,13]. In annular (A) and intermittent (I), $\theta_{dry} = 0$. For stratified-wavy flow, θ_{dry} varies from zero up to its maximum value θ_{strat}. Stratified-wavy flow has been subdivided into three subzones (slug, slug/stratified-wavy, and stratified-wavy) to determine θ_{dry}. For slug zone (Slug), the high frequency slugs maintain a continuous thin liquid layer on the upper tube perimeter. Thus, similar to the intermittent and annular flow re-

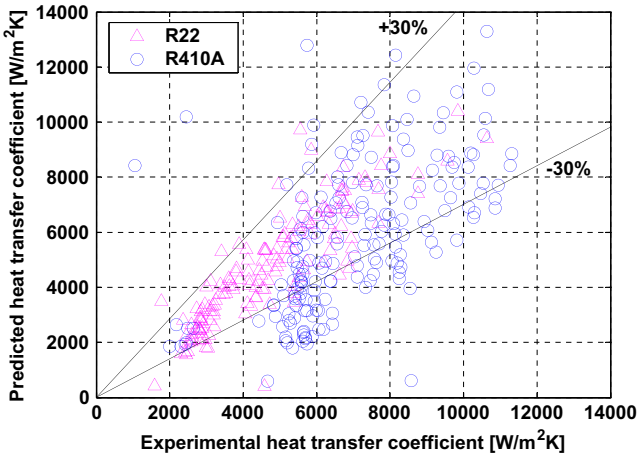

Fig. 6. Comparison of the entire experimental heat transfer coefficient to the predicted results by the Wojtan et al. [12,13] heat transfer model for R22 and R410A.

Table 2
Statistical analysis of the predicted flow boiling heat transfer coefficients for R22 and R410A by the heat transfer model of Wojtan et al. [12,13].

Data used for comparison	Experimental data points	Percentage of predicted points (relative error ξ) within ±30%	Mean error, $\lvert\bar{\xi}\rvert$	Standard deviation, σ
Slug-SW	18	22.2%		
SW	10	40%		
I+Slug	139	66.2%		
Annular flow	153	88.9%		
Dryout region	30	53.3%		
Mist flow	5	0		
All data points	355	71%	24.1%	33.8%

gimes, $\theta_{dry} = 0$. The calculation of the dry angle for other flow regimes can be found in [12,13].

The vapor phase heat transfer coefficient on the dry perimeter h_V is calculated with the Dittus–Boelter [25] correlation assuming tubular flow:

$$h_V = 0.023\, Re_V^{0.8}\, Pr_V^{0.4}\, \frac{k_V}{D_e}, \tag{4}$$

Where the vapor phase Reynolds number Re_V is defined as

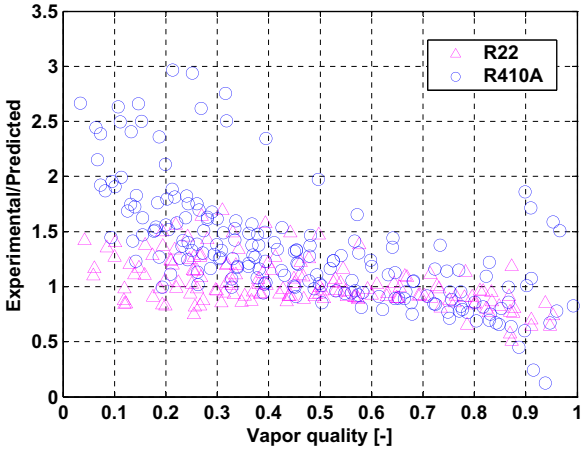

Fig. 7. Experimental and predicted flow boiling heat transfer coefficient ratios versus vapor qualities for R22 and R410A.

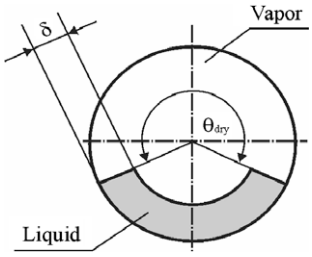

Fig. 8. Schematic diagram of film thickness.

$$Re_V = \frac{GxD_e}{\mu_V \varepsilon}. \tag{5}$$

The heat transfer coefficient on the wet perimeter h_{wet} is calculated with an asymptotic model that combines the nucleate boiling and convective boiling heat transfer contributions to flow boiling heat transfer by the third power:

$$h_{wet} = \left[(Fh_{nb})^3 + h_{cb}^3\right]^{1/3}, \tag{6}$$

where h_{nb}, F, and h_{cb} are, respectively, the nucleate boiling heat transfer coefficient, the nucleate boiling heat transfer correction factor and the convective boiling heat transfer coefficient, where $F = 0.8$ for circular tubes.

The nucleate boiling heat transfer coefficient h_{nb} is calculated with the Cooper [26] correlation:

$$h_{nb} = 55 p_r^{0.12} (-\log_{10} p_r)^{-0.55} M^{-0.5} q^{0.67}. \tag{7}$$

For the flattened tubes, the factor F is corrected considering the nucleate boiling heat transfer contribution due to the effect of confinement of the flat tube heights (the equivalent diameter D_e combines this effect) in stratified-wavy and slug, slug, and intermittent flow regimes when vapor qualities x lower than x_{IA}, and the thinning of the annular liquid film:

$$\text{If } x \le x_{IA}, \quad F = 0.8 + 2.46\left(\frac{\delta}{\delta_{IA}} - 1\right)^{0.17}\left(\frac{p_r}{0.12} - 1\right)^2, \tag{8}$$

$$\text{If } x > x_{IA}, \quad F = 0.8, \tag{9}$$

and the liquid film thickness δ shown in Fig. 8 is calculated with the expression proposed by El Hajal et al. [27]:

$$\delta = \frac{D_e}{2} - \sqrt{\left(\frac{D_e}{2}\right)^2 - \frac{2A_L}{2\pi - \theta_{dry}}}, \tag{10}$$

where A_L, based on the equivalent diameter, is cross-sectional area occupied by liquid phase. When the liquid occupies more than one-half of the cross-section of the tube at low vapor quality, this expression would yield a value of $\delta > D_e/2$, which is not geometrically realistic. Hence, whenever Eq. (10) gives $\delta > D_e/2$, δ is set equal to $D_e/2$ (occurs when $\varepsilon < 0.5$). The correction factor correlation gives a value of 0.8 for R22 when the reduced pressure p_r equals 0.12, which is the original value used in the Wojtan et al. model. The correction factor is applied to the reduced pressures up to 0.19.The convective boiling heat transfer coefficient h_{cb} is calculated with the following correlation assuming an annular liquid film flow from the original model [11]:

$$h_{cb} = 0.0133\, Re_\delta^{0.69}\, Pr_L^{0.4}\, \frac{k_L}{\delta}, \tag{11}$$

where the liquid film Reynolds number Re_δ is defined as [11]

$$Re_\delta = \frac{4G(1-x)\delta}{\mu_L(1-\varepsilon)}. \tag{12}$$

The void fraction ε is calculated with Eq. (12) in paper Part I and δ is calculated with Eq. (10).

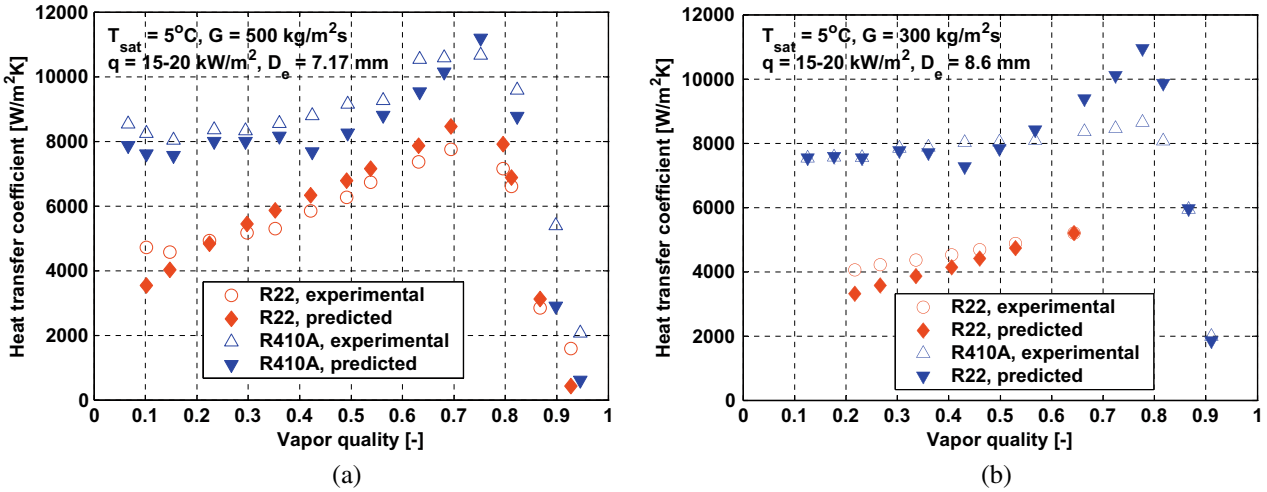

Fig. 9. Comparison of the experimental heat transfer coefficients to the predicted results by the modified heat transfer model for R22 and R410A at the indicated conditions: (a) Tube No. 1 and (b) Tube No. 2.

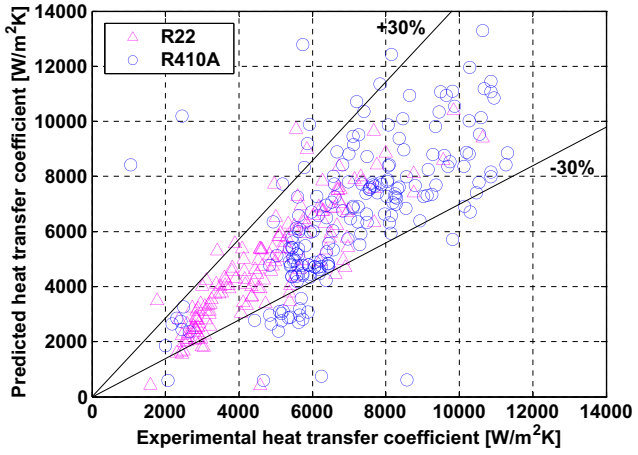

Fig. 10. Comparison of the entire experimental heat transfer coefficient to the predicted results by the modified heat transfer model for R22 and R410A.

Fig. 9 shows the comparison of the modified heat transfer model to the selected test runs of R22 and R410A in Tube No. 1 and No. 2. It can be seen that the modified flow boiling heat transfer model not only captures the heat transfer trends well but also predicts the experimental heat transfer data well. Fig. 10 shows the comparison of the entire R22 and R410A database to the modified model, with 85.8% of the data points predicted within ±30%. In further analysis, comparisons have also been made according to flow regimes in Table 3. The predictions in the slug-stratified wavy (Slug-SW) and stratified wavy (SW) flow regimes are improved while the predictions in dryout and mist flow regimes are not satisfactory. As already mentioned, the flow regime observations were not made in the present study and, therefore, errors in flow regime identification might be one of the main reasons why the experimental data are sometimes not well predicted. Therefore, flow visualization in the flattened tubes is suggested to be performed to improve the heat transfer model when a safe method is available in the future. At this stage, the predicted results seem reasonable as most of the present data are in the intermittent and annular flow regimes.

Table 3
Statistical analysis of the predicted flow boiling heat transfer coefficients for R22 and R410A by the modified heat transfer model.

Data used for comparison	Experimental data points	Percentage of predicted points (relative error ξ) within ±30%	Mean error, $\|\bar{\xi}\|$	Standard deviation, σ
Slug-SW	18	61.1%		
SW	10	70%		
I+Slug	139	96.4%		
Annular flow	153	88.9%		
Dryout region	30	53.3%		
Mist flow	5	0		
All data points	355	85.6%	17.7%	30.5%

5. Conclusions

Experiments of flow boiling heat transfer of R22 and R410A were conducted in four horizontal flattened copper smooth tubes with two different heights of 2 and 3 mm for mass velocities from 150 to 500 kg/m^2 s, heat fluxes from 6 to 40 kW/m^2 and a saturation temperature of 5 °C. From the present study, the following conclusions are obtained (most of which are very similar to those of round tubes):

(1) Mass flux has a significant effect on the flow boiling heat transfer coefficients at larger vapor qualities while this effect becomes insignificant at very lower vapor qualities. This is because convective boiling is the dominant heat transfer mechanism at large vapor qualities and nucleate boiling is the dominant heat transfer mechanism at low vapor qualities.
(2) Mass flux has a significant effect on the onset of dryout. Normally, the onset of dryout occurs earlier at a higher mass flux.
(3) Heat flux has a significant effect on the flow boiling heat transfer coefficients. This effect becomes stronger at lower vapor qualities because nucleate boiling is the dominant heat transfer mechanism. Furthermore, heat flux has a great effect on the location of the onset of dryout. Dryout occurs earlier at higher heat fluxes.
(4) The equivalent diameter has an effect on flow boiling heat transfer coefficients, which increase with decreasing equivalent diameter. This effect may attribute to the confined function of the small flattened tube heights.
(5) The flow pattern based flow boiling heat transfer model of Wojtan et al. predicted 71% of the flattened tube heat transfer coefficients of R22 and R410A within ±30% overall. The model works well for R22 while it does not work well for R410A.

(6) A modified flow boiling heat transfer model was proposed for the flattened tubes. The model is applied to the reduced pressures up to 0.19.The model improved the prediction for the entire R22 and R410A database from 71% to 85.8% within ±30% overall. However, in some flow regimes, the predictions are not satisfactory, which might be caused by flow regime identification errors. Therefore, flow visualization in the flattened tubes should be performed to improve the model when a safe method is available in the future.

Acknowledgements

The Laboratory of Heat and Mass Transfer (LTCM) at the École Polytechnique Fédérale de Lausanne (EPFL) wishes to thank ARTI for sponsoring this project with contract ARTI-21CR/605-20040-01. LTCM wishes to also thank Wolverine Tube Inc. for providing the extruded flat tubes for the tests.

References

[1] M.J. Wilson, T.A. Newell, J.C. Chato, C.A. Infante Ferreira, Refrigerant charge pressure drop and condensation heat transfer in flattened tubes, Int. J. Refrigeration 26 (2003) 442–451.
[2] S. Krishnaswamy, H.S. Wang, J.W. Rose, Condensation from gas–vapor mixtures in small non-circular tubes, Int. J. Heat Mass Transfer 49 (2006) 1731–1737.
[3] S. Koyama, K. Kuwahara, K. Nakashita, K. Yamamoto, An experimental study on condensation of refrigerant R134a in a multi-port extruded tube, Int. J. Refrigeration 24 (2003) 425–432.
[4] L. Cheng, D. Mewes, A. Luke, Boiling phenomena with surfactants and polymeric additives: a state-of-the-art review, Int. J. Heat Mass Transfer 50 (2007) 2744–2771.
[5] J.R. Thome, Boiling in microchannels: a review of experiment and theory, Int. J. Heat Fluid Flow 25 (2004) 128–139.
[6] L. Cheng, D. Mewes, Review of two-phase flow and flow boiling of mixtures in small and mini channels, Int. J. Multiphase Flow 32 (2006) 183–207.
[7] S.G. Kandlikar, Fundamental issues related to flow boiling in minichannels and microchannels, Exp. Therm. Fluid Sci. 26 (2002) 389–407.
[8] L. Cheng, G. Ribatski, J.R. Thome, Gas–liquid two-phase flow patterns and flow pattern maps: fundamentals and applications, ASME Appl. Mech. Rev. 61 (2008) 050802-1–050802-28.
[9] N. Kattan, J.R. Thome, D. Favrat, Flow boiling in horizontal tubes. Part 1: Development of a diabatic two-phase flow pattern map, J. Heat Transfer 120 (1998) 140–147.
[10] N. Kattan, J.R. Thome, D. Favrat, Flow boiling in horizontal tubes: Part 2 – New heat transfer data for five refrigerants, J. Heat Transfer 120 (1998) 148–155.
[11] N. Kattan, J.R. Thome, D. Favrat, Flow boiling in horizontal tubes: Part-3: Development of a new heat transfer model based on flow patterns, J. Heat Transfer 120 (1998) 156–165.
[12] L. Wojtan, T. Ursenbacher, J.R. Thome, Investigation of flow boiling in horizontal tubes: Part I – A new diabatic two-phase flow pattern map, Int. J. Heat Mass Transfer 48 (2005) 2955–2969.
[13] L. Wojtan, T. Ursenbacker, J.R. Thome, Investigation of flow boiling in horizontal tubes: Part II – Development of a new heat transfer model for stratified-wavy, dryout and mist flow regimes, Int. J. Heat Mass Transfer 48 (2005) 2970–2985.
[14] L. Cheng, G. Ribatski, L. Wojtan, J.R. Thome, New flow boiling heat transfer model and flow pattern map for carbon dioxide evaporating inside horizontal tubes, Int. J. Heat Mass Transfer 49 (2006) 4082–4094.
[15] L. Cheng, G. Ribatski, L. Wojtan, J.R. Thome, Erratum to: "New flow boiling heat transfer model and flow pattern map for carbon dioxide evaporating inside tubes" [Heat Mass Transfer 49 (21–22) (2006) 4082–4094], Int. J. Heat Mass Transfer 50 (2007) 391.
[16] L. Cheng, G. Ribatski, J. Moreno Quibén, J.R. Thome, New prediction methods for CO_2 evaporation inside tubes: Part I – A two-phase flow pattern map and a flow pattern based phenomenological model for two-phase flow frictional pressure drops, Int. J. Heat Mass transfer 51 (2008) 111–124.
[17] L. Cheng, G. Ribatski, J.R. Thome, New prediction methods for CO_2 evaporation inside tubes: Part II – An updated general flow boiling heat transfer model based on flow patterns, Int. J. Heat Mass transfer 51 (2008) 125–135.
[18] R.J. da Silva Lima, J. Moreno Quibén, J.R. Thome, Flow boiling in horizontal smooth tube: new heat transfer results for R134a at three saturation temperatures, Appl. Therm. Eng. 29 (2009) 1289–1298.
[19] R.J. da Silva Lima, J. Moreno Quibén, C. Kuhn, T. Boyman, Ammonia two-phase flow in a horizontal smooth tube: flow pattern observations, diabatic and adiabatic frictional pressure drops and assessment of prediction methods, Int. J. Heat Mass Transfer 52 (2009) 2273–2288.
[20] REFPROP, NIST Refrigerant Properties Database 23, Gaithersburg, MD, 1998, Version 6.01.
[21] J. Bonjour, M. Lallemand, Effects of confinement and pressure on critical heat flux during natural convective boiling in vertical channels, Int. Comm. Heat Mass Transfer 24 (1997) 191–200.
[22] J. Bonjour, M. Lallemand, Flow patterns during boiling in a narrow space between two vertical surfaces, Int. J. Multiphase Flow 24 (1998) 947–960.
[23] J. Yu, S. Momoki, S. Koyama, Experimental study of surface effect on flow boiling heat transfer in horizontal smooth tubes, Int. J. Heat Mass Transfer 42 (1999) 1909–1918.
[24] J.R. Thome, V. Dupont, A.M. Jacobi, Heat transfer model for evaporation in microchannels. Part I. Presentation of the model, Int. J. Heat Mass Transfer 47 (2004) 3375–3385.
[25] F.W. Dittus, L.M.K. Boelter, Heat transfer in automobile radiator of the tubular type, Univ. Calif. Publ. Eng. 2 (1930) 443–461.
[26] M.G. Cooper, Saturation nucleate pool boiling: a simple correlation, in: Proc. of the 1st UK National Conference on Heat Transfer, vol. 2, pp. 785–793.
[27] J. El Hajal, J.R. Thome, A. Cavallini, Condensation in horizontal tubes, Part 2: New heat transfer model based on flow regimes, Int. J. Heat Mass Transfer 46 (2003) 3365–3387.